

Local Information Matters: Inference Acceleration For Grounded Conversation Generation Models Through Adaptive Local-Aware Token Pruning

Bizhe Bai^{1,2} Jianjian Cao¹ Yadan Luo³ Tao Chen^{1,2*}

¹Fudan University ²Shanghai Innovation Institute

³The University of Queensland

eet.chen@fudan.edu.cn

Abstract

*Grounded Conversation Generation (GCG) is an emerging vision-language task that requires models to generate natural language responses seamlessly intertwined with corresponding object segmentation masks. Recent models, such as GLaMM and OMG-LLaVA, achieve pixel-level grounding but incur significant computational costs due to processing a large number of visual tokens. Existing token pruning methods, like FastV and PyramidDrop, fail to preserve the local visual features critical for accurate grounding, leading to substantial performance drops in GCG tasks. To address this, we propose **Adaptive Local-Aware Token Pruning (ALTP)**, a simple yet effective framework that accelerates GCG models by prioritizing local object information. ALTP introduces two key components: (1) **Detail Density Capture (DDC)**, which uses superpixel segmentation to retain tokens in object-centric regions, preserving fine-grained details, and (2) **Dynamic Density Formation (DDF)**, which dynamically allocates tokens based on information density, ensuring higher retention in semantically rich areas. Extensive experiments on the GrandF dataset demonstrate that ALTP significantly outperforms existing token pruning methods, such as FastV and PyramidDrop, on both GLaMM and OMG-LLaVA models. Notably, when applied to GLaMM, ALTP achieves a 90% reduction in visual tokens with a 4.9% improvement in AP50 and a 5.0% improvement in Recall compared to PyramidDrop. Similarly, on OMG-LLaVA, ALTP improves AP by 2.1% and mIOU by 3.0% at a 90% token reduction compared with PDrop.*

1. Introduction

Grounded Conversation Generation (GCG) is an emerging vision-language task in which a model must produce textual responses accompanied by segmentation masks for specific

regions of an image [22]. For example, a GCG model might generate the sentence “The bed is positioned beside the wall. A curtain is hanging from the wall,” while also providing segmentation masks that precisely outline the bed, wall, and curtain. Compared to traditional vision-language tasks such as image captioning or visual question answering (VQA) [5, 6, 14, 20, 25], which only output text, or referring segmentation tasks [7, 11, 26], which only predict segmentation masks for a given query phrase, GCG explicitly requires the model to produce holistic descriptions that interleave object mentions with their corresponding masks. This capability is vital for applications requiring precise visual reasoning, such as interactive agents that can identify objects in real-time or systems that generate detailed instructions for image editing.

Recently, Rasheed *et al.* introduced GLaMM [22], the first large-scale model for GCG, demonstrating the feasibility of pixel-level grounding within multimodal conversations. OMG-LLaVA [30] followed with a more compact architecture, achieving higher accuracy without relying on additional segmentation models like SAM [9]. Both approaches generate complete image descriptions intertwined with segmentation masks (dense grounding) by processing a substantial number of visual tokens. For example, GLaMM employs 576 visual tokens per image, while OMG-LLaVA uses 256. Although these models achieve fine-grained accuracy, they incur substantial computational overhead. Since both are built upon the LLaVA framework [14], one might consider existing token-pruning methods such as FastV [4] or PyramidDrop [27] to reduce this cost. However, when we applied FastV directly to GLaMM and OMG-LLaVA, the performance on GCG tasks dropped significantly. For instance, Figure 2(a)–(c) shows that pruning 75% of GLaMM’s visual tokens with FastV cut its recall by half, from 0.8 to 0.4. By contrast, using the same pruning ratio in text-focused multimodal tasks (e.g., MMMU [28] or A-OKVQA [17]) reduced performance by only about 2%. We hypothesize that GCG tasks demand more localized visual features than traditional VQA or captioning tasks. In-

*Corresponding Author: eet.chen@fudan.edu.cn



Figure 1. (a): Result of original GLaMM [22]. (b): Result of GLaMM with Fastv [4] method pruning 90% of visual token starting from the second layer. (c) : Result from GLaMM with Fastv method pruning 75% of visual tokens starting from the second layer. (d): Results from GLaMM using FastV [4] with 90% visual token pruning and retaining additional visual tokens retained at the curtain location, starting from the second layer. Comparing (c) and (d), we could conclude that **“Local Information Matters”**: preserving visual tokens corresponding to object locations provides richer object information to the vision-language model.

inspired by Pan *et al.* [18], who showed that global attention struggles to capture local details in vision transformers, we further tested whether reintroducing tokens corresponding to small, salient objects (e.g., a curtain) could restore GCG performance. Indeed, selectively retaining these local tokens not only recovered lost accuracy but sometimes surpassed the performance of less aggressive pruning schemes (Figure 2(d)).

Drawing on these observations, we propose a novel token-pruning approach tailored for GCG models. Rather than relying exclusively on global cross-attention to identify redundant tokens, our framework explicitly preserves tokens that encode local, object-centric information. Concretely, we make three key contributions:

- We highlight why standard token-pruning methods struggle in GCG tasks, emphasizing the importance of local visual features in grounded conversation.
- We propose a simple yet effective framework that combines superpixel segmentation with an adaptive token-allocation strategy, ensuring critical object-level details are retained.

- Through extensive experiments on the GrandF dataset, we demonstrate that our method significantly outperforms existing token-pruning approaches (FastV, PyramidDrop) on both GLaMM and OMG-LLaVA, reducing token counts by up to 90% while improving segmentation and recall metrics.

2. Related Work

2.1. Multimodal Large Language Models

The field of Multimodal Large Language Models (MLLMs) has witnessed explosive growth in recent years, driven by advancements in deep learning and the increasing availability of multimodal datasets. Early works like Flamingo [2] and BLIP-2 [12] leveraged pre-trained vision encoders and LLMs, connected via lightweight adapters, to achieve impressive performance on tasks like image captioning and visual question answering. In contrast, LLaVA [13] and LLaVA-1.5 [15] employ the MLP layer to directly map encoded visual features into the input embedding space of the LLM, significantly simplifying both the model architecture

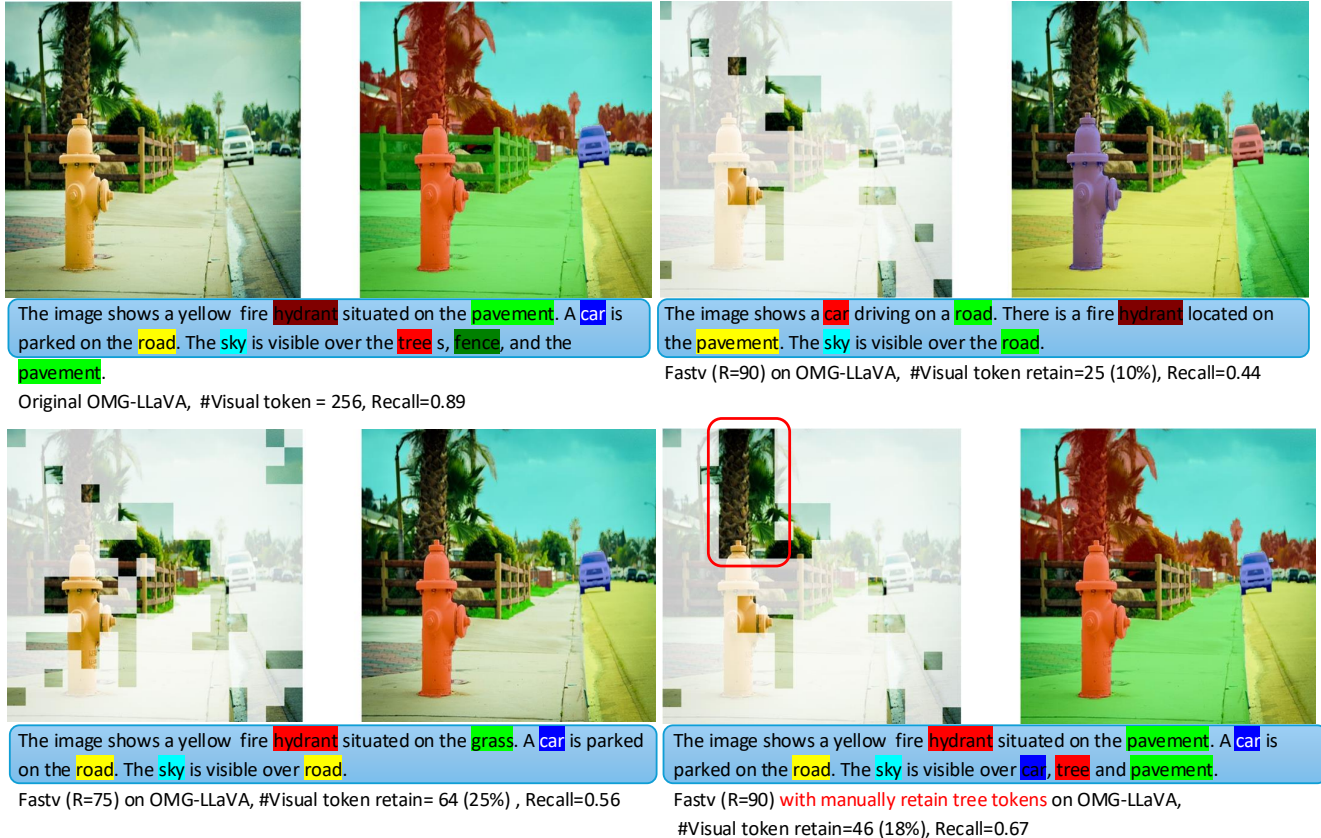


Figure 2. (a): Result of original OMG-Llava [30]. (b): Result of OMG-Llava with Fastv [4] method pruning 90% of visual token starting from the second layer. (c) Result of pruning 75% of visual tokens starting from the second layer. (d) Pruning 90% visual token pruning and retaining additional visual tokens retained at the tree location. Comparing (c) and (d), we can conclude the same conclusion as Figure 2: “Local Information Matters” .

and training pipeline. Despite these advancements, most existing MLLMs are primarily designed to generate textual outputs from multimodal inputs but lack the capability to predict object masks in images, limiting their effectiveness in fine-grained visual understanding tasks.

2.2. Grounded Conversation Generation

Recent research in GCG task has focused on enabling region-specific dialogue by integrating spatial and visual information with language models. Several notable works [3, 19, 24, 29] have explored methods to facilitate fine-grained, region-level understanding in multimodal conversations. These approaches typically incorporate location bins, bounding boxes, or spatial coordinates alongside image data to enhance the model’s ability to interpret and reason about specific regions within an image. For instance, methods like Shikra [3] and Kosmos-2 [19] rely on large language models (LLMs) to process region-specific inputs, such as bounding boxes, and generate corresponding textual descriptions. GPT4RoI [29] advances this paradigm by incorporating spatial boxes and region-of-interest (RoI)-aligned features as inputs, training on region-text pairs to improve alignment between visual regions and

textual outputs. Similarly, BuboGPT [32] leverages an off-the-shelf grounding model [16] to align visual groundings with language responses, enabling more precise region-aware dialogue generation. In contrast, LISA [10] utilizes embeddings from a vision-language model combined with the Segment Anything Model (SAM) [9] decoder to generate segmentation masks as outputs. More recently, GLaMM [22] has demonstrated the feasibility of pixel-level grounding in visual-language conversations, enabling fine-grained understanding of images. Building on this, OMG-LLaVA [30] proposed a more streamlined framework, achieving superior accuracy without relying on external segmentation models like SAM [9]. While these methods have shown impressive results, they often come with significant computational costs due to their reliance on large-scale models. To address this limitation, our work focuses on accelerating these GCG models, enabling faster inference while maintaining performance.

2.3. Token Pruning for Vision-Language Models

The visual tokens show more redundancy than text-tokens in visual-language models [4]. Recently, there is a growing number of work on accelerating vision-language mod-

els (VLM) by reducing the number of visual tokens fed into the language model. One class of approaches prunes tokens based on their importance scores. In the context of llava-like VLMs, a common heuristic is to use the cross-attention between visual tokens and textual inputs: tokens that a language model attends to weakly are assumed less important and can be dropped. These works such as FastV [4], LLaVA-PruMerge [23] and PyramidDrop [27]. FastV is a notable example of this strategy. FastV [4] learns to prune visual tokens in the early layers of a vision-language model by identifying those tokens that have low attention impact on the text tokens. Some other token pruning methods used the input text to explicitly guide the visual token pruning and achieve better results.[31, 33]. We diverge from prior approaches by explicitly accounting for each object’s local visual information therefore insure the object information is indeed flowed inside the visual language model.

3. Methodology

The architecture overview is depicted in Figure 3. In the following, we first give a brief introduction of the Visual-language model and Grounded Conversation Generation in Section 3.1. Then, we present our Adaptive Local-Aware Token Pruning modules in Section 3.2 and Section 3.3. Finally, we present the overall pruning pipeline in Section 3.4.

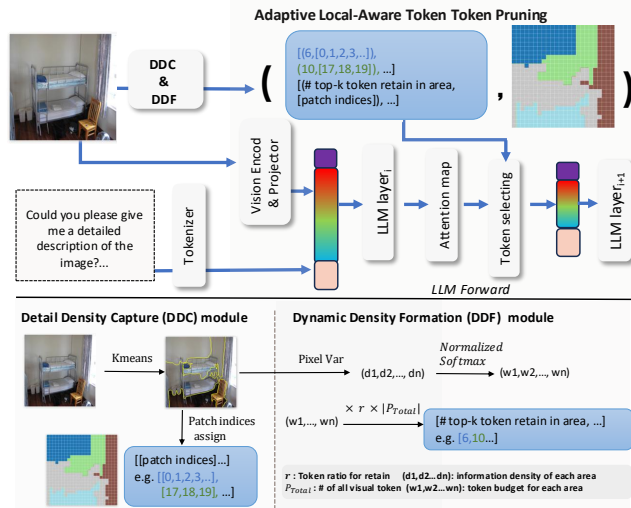


Figure 3. Overview of the proposed Adaptive Local-Aware Token Pruning (ALTP) framework. It comprises two main components: the Detail Density Capture (DDC) module and the Dynamic Density Formation (DDF) module. The DDC module segments the image into semantically coherent sub-areas, ensuring that a larger proportion of tokens corresponding to the location of detail density regions will be retained for precise pixel-level grounding. Meanwhile, the DDF module dynamically adjusts token allocation within each region based on information density, allowing for an adaptive pruning strategy that ensuring higher token retention for tokens rich in detail.

3.1. Preliminaries

Visual Language Models. Large Visual Language Models (LVLMs) are multimodal foundation models that combine visual perception capabilities with language understanding and generation. These models typically consist of three key components: (1) a visual encoder that transforms images into visual token representations, (2) a projector that aligns the visual tokens with the text embedding space, and (3) a large language model (LLM) backbone that processes the combined visual and textual information to generate responses [14]. Formally, given an image I and a text prompt P , an LVLM processes the input as follows:

$$Res = LLM(\mathbf{Z}_v \oplus E_{\text{text}}(P)), \text{ with } \mathbf{Z}_v = Proj(g(\mathbf{X}_v)), \quad (1)$$

where g is the visual encoder, usually a Clip model [21], \mathbf{X}_v is the input image, E_{text} is the text tokenizer and embedding layer, $Proj$ is the vision projection layer, usually a MLP Layer, \oplus denotes the concatenation operation, and Res is the generated response. LVLMs excel at tasks such as image captioning, visual question answering, and multimodal reasoning, but they typically produce free-form text without explicit grounding to specific regions in the image.

Grounded Conversation Generation Grounded Conversation Generation (GCG) extends the capabilities of traditional LVLMs by requiring the model to not only generate textual responses based on visual input but also to explicitly ground textual phrases to specific regions within the image. A GCG model takes an image I and a prompt P , which a sample prompt is like “Could you please give me a detailed description of the image? Please respond with interleaved segmentation masks for the corresponding parts of the answer.” as input and generates a holistic caption along with interleaved segmentation mask response R along with a set of segmentation masks M_1, M_2, \dots, M_k corresponding to specific phrases S_1, S_2, \dots, S_k within the response, employing the format The $\langle p \rangle$ bed $\langle /p \rangle$ $\langle \text{SEG} \rangle$ is positioned beside the $\langle p \rangle$ wall $\langle /p \rangle$ $\langle \text{SEG} \rangle$. A $\langle p \rangle$ curtain $\langle /p \rangle$ $\langle \text{SEG} \rangle$ is hanging from the $\langle p \rangle$ wall $\langle /p \rangle$ $\langle \text{SEG} \rangle$. In GCG task, the start and end of each phrase and its corresponding region mask usually represent by special tokens, namely $\langle p \rangle, \langle /p \rangle$ and $\langle \text{SEG} \rangle$, respectively. The segmentation result is decoded from last-layer embeddings corresponding to the $\langle \text{SEG} \rangle$ tokens. In Glamm, its decoder is a SAM-like [9] architecture decoder. In OMG-Llava, its decoder is comprises with cross-attention and self-attention layers, it generates the segmentation result with $\langle \text{SEG} \rangle$ tokens’ embedding and image features.

3.2. Detail Density Capture (DDC)

To retain critical local features, we propose a **Detail Density Capture** (DDC) module that segments the image into sub-regions and treats each sub-region as a unit for token

pruning. Empirically, we observe that standard global attention methods tend to overlook subtle object boundaries, causing significant performance drops in GCG.

Superpixel-Based Sub-Regions. We employ superpixel segmentation (via SLIC [1]) to divide the image \mathbf{X}_v into K visually coherent regions:

$$\{\mathcal{S}_1, \mathcal{S}_2, \dots, \mathcal{S}_K\} = \Phi_{\text{SLIC}}(\mathbf{X}_v; N, C, \sigma), \quad (2)$$

where N is the target number of superpixels, C controls compactness (i.e., trade-off between color and spatial proximity), and σ is a Gaussian smoothing parameter. For each \mathcal{S}_k , we identify the set of tokens that correspond to pixels within that superpixel. Instead of pruning solely based on global criteria, DDC ensures that each superpixel region retains at least a fraction of its tokens, thus preserving fine-grained features critical to describing local objects (e.g., “wall,” “curtain,” etc.).



The image shows a **bed** room with a **chair**, a **backpack** and a **table** placed on the wooden floor. A **wall** is also visible in the room.

Detail Density Capture token pruning(R=75) on Glamm,
#Visual token retain= 144, Recall=0.6

Figure 4. Detail Density Capture (DDC) visualization. Left: Retained token locations using DDC with a 75% token drop. Right: Grounded conversation generation result using DDC, demonstrating successful generation of the “wall” phrases and mask.

Pruning Within Each Sub-Region. Let Ω_k be the set of visual-token indices corresponding to superpixel \mathcal{S}_k . We maintain a local keep-ratio r_k for each region. If $|\Omega_k|$ is the number of tokens in region k , we keep $\lceil r_k \cdot |\Omega_k| \rceil$ tokens. The simplest version of DDC sets r_k identically for all k , ensuring uniform retention across sub-regions. However, uniform distribution still may not reflect varying complexity among objects (e.g., large uniform backgrounds vs. small, detail-rich objects). This motivates our second module, DDF, to allocate tokens *dynamically*.

3.3. Dynamic Density Formation (DDF)

Although DDC preserves local features, it treats each region equally. In practice, large objects (e.g., walls) may not require as many tokens as smaller, high-detail objects (e.g.,

a lamp with intricate shapes). Hence, we introduce a **Dynamic Density Formation (DDF)** strategy to allocate the overall token budget proportionally to a region’s *information density*.

Information Density. For each superpixel \mathcal{S}_k , we define an *information density* d_k that combines pixel variance and area size:

$$d_k = \text{Var}(\mathcal{S}_k) \sqrt{\frac{|\mathcal{P}_k|}{|\mathcal{P}_{\text{total}}|}}, \quad (3)$$

where $\text{Var}(\mathcal{S}_k)$ is the color variance within region k , $|\mathcal{P}_k|$ is the number of pixels (or patches) in \mathcal{S}_k , and $|\mathcal{P}_{\text{total}}|$ is the total number of pixels in the entire image. The multiplier $\sqrt{\frac{|\mathcal{P}_k|}{|\mathcal{P}_{\text{total}}|}}$ prevents extremely small but high-variance regions from dominating the token budget.

Token Allocation. Given a total keep-ratio r for visual tokens, we wish to distribute these tokens among the K superpixels proportionally to d_k . We first compute normalized weights w_k via a softmax-like mechanism:

$$w_k = \frac{\exp\left(\frac{d_k}{\alpha \cdot \max(d)}\right)}{\sum_{j=1}^K \exp\left(\frac{d_j}{\alpha \cdot \max(d)}\right)}, \quad (4)$$

where $\alpha > 1$ is a scaling factor (e.g., $\alpha = 1.5$) to avoid overly skewed allocations. Then, if V_{total} is the initial number of visual tokens, we allocate:

$$T_k = w_k \times (r \cdot V_{\text{total}})$$

tokens to superpixel \mathcal{S}_k . Concretely, we keep the top $\lceil T_k \rceil$ tokens (by some local importance criterion, e.g. cross-attention or self-attention magnitude) within that superpixel. Figure 5 shows that DDF adaptively allocates more tokens to high-detail objects (e.g., a curtain), improving segmentation accuracy compared to uniform allocation.

3.4. Overall Pruning Pipeline

Algorithm 1 summarizes our full approach. We first generate superpixels via DDC (Eq. 2), then compute d_k for each sub-region (Eq. 3). We convert d_k into allocation weights w_k (Eq. 4) and select tokens accordingly. This pruned set of tokens is concatenated with the text embedding and fed into the language model.

By combining DDC and DDF, our ALTP framework ensures that tokens corresponding to high-detail or semantically rich objects are preserved, while uniform or low-detail areas are pruned aggressively.

Algorithm 1 Adaptive Local-Aware Token Pruning (ALTP)

Require: Image \mathbf{X}_v , Prompt \mathbf{P} , Total Keep-Ratio r , Number of Superpixels N , Compactness C

- 1: // **Step 1: DDC**
 - 2: $\{\mathcal{S}_1, \dots, \mathcal{S}_K\} \leftarrow \Phi_{\text{SLIC}}(\mathbf{X}_v; N, C, \sigma)$
 - 3: **for** $k = 1$ to K **do**
 - 4: Identify token indices Ω_k of \mathcal{S}_k
 - 5: **end for**
 - 6: // **Step 2: DDF**
 - 7: **for** $k = 1$ to K **do**
 - 8: Compute $d_k = \text{Var}(\mathcal{S}_k) \sqrt{\frac{|\mathcal{P}_k|}{|\mathcal{P}_{\text{total}}|}}$
 - 9: **end for**
 - 10: Compute w_k using Eq. (4) for $k = 1, \dots, K$
 - 11: // **Step 3: Token Selection**
 - 12: $V_{\text{total}} \leftarrow$ total # of visual tokens from Enc_v
 - 13: **for** $k = 1$ to K **do**
 - 14: $T_k \leftarrow w_k \times (r \cdot V_{\text{total}})$
 - 15: Keep top $\lceil T_k \rceil$ tokens in Ω_k based on local importance
 - 16: **end for**
 - 17: $\Omega_{\text{selected}} \leftarrow \bigcup_{k=1}^K$ (kept tokens in Ω_k)
 - 18: // **Step 4: Inference**
 - 19: Forward $E_{\text{text}}(\mathbf{P}) \oplus \text{Proj}(\text{Enc}_v(\Omega_{\text{selected}}))$ to LLM
-

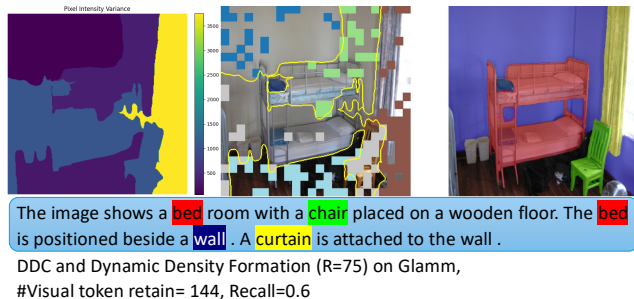


Figure 5. Visualization of Dynamic Density Formation (DDF) token allocation. **Left:** Pixel variance for each sub-area calculated using Equation 3, indicating higher information density in regions like the curtain. **Middle:** Corresponding token allocation weights derived from information density via Equation 4, showing that tokens in regions with higher variance (e.g., the curtain) receive a larger allocation budget. **Right:** Final generation results with the DDC and DDF modules under a 25% token allocation setting. Compared to uniform token allocation in DDC as shown in Figure 4, the DDF module enables the model to dynamic allocate token budge to the tokens with more information density, therefore, capture and generate detailed objects (e.g., the curtain).

4. Experiment results

4.1. Experimental Setup

Datasets and Evaluation Metrics. We evaluate our proposed token pruning method on two state-of-the-art Grounded Conversation Generation (GCG) models: Glamm [22] and OMG-Llava [30]. Experiments are conducted us-

ing the GrandF dataset, the only established benchmark for GCG, with 2.5K validation and 5K test samples. Performance is assessed using : METEOR and CIDEr for captioning quality, AP50, mask Intersection over Union (IoU) for segmentation mask, and mask recall for evaluating region-specific grounding. The recall calculation follows that of GlaMM, counting a “hit” only if the generated mask and phrase pair surpass both 0.5 IoU and 0.5 BERT similarity thresholds with respect to the ground-truth mask and phrases.

FLOPS estimated For one transformer layer with multi-head attention and feed-forward network (FFN), assume n is the token number, d is the hidden state size, m is the intermediate size of FFN, the total FLOPs can be estimated by $f_l(n) = 4nd^2 + 2n^2d + 2ndm$. For the whole model, assume pruning tokens from n to $\hat{n} = (1 - R\%) \cdot n$ after layer K and there are T layers all. The theoretical FLOPs reduction ratio related to image tokens is computed as:

$$1 - \frac{K \times f_l(n) + (T - K) \times f_l(\hat{n})}{T \times f_l(n)} \quad (5)$$

Comparison Methods. We benchmark our proposed token pruning method against existing state-of-the-art methods, including FastV [4] and PDrop [27]. The choice is driven by two three factors. First, other widely-used datasets such as refCOCO, refCOCO+, and refCOCOG [8] are primarily designed for text-driven segmentation tasks, where the model outputs a segmentation mask based solely on a given query text, disregarding phrase generation. Moreover, state-of-the-art methods on these datasets, such as LISA [10], generate segmentation masks directly through decoding special tokens (e.g., $\langle \text{SEG} \rangle$ tokens) in a non-autoregressive manner, fundamentally differing from Grounded Conversation Generation (GCG) models like Glamm, which produce both phrases and segmentation masks auto-regressively. Consequently, such datasets and models are not directly comparable with GCG models. Second, our proposed ALTP method specifically targets visual token pruning in large visual-language models architecturally similar to Llava. Lastly, some other token pruning methods used the relevant text in query to explicitly guide the visual token pruning and achieve better results.[31, 33]. These methods do not fit the GCG task because the input text of GrandF dataset does not have relevant text information that could benefit token pruning. A sample query is “Could you please give me a detailed description of the image? Please respond with interleaved segmentation masks for the corresponding parts of the answer.” Thus, our experimental comparison appropriately focuses on methods aligned with this scenario.

4.2. Experiments on GCG task

ALTP excels with Glamm on GrandF dataset As Table 1 presents the performance of our proposed ALTP method

Model name	FLOPS	Val					Test				
		METEOR	CIDEr	AP50	mIOU	Recall	METEOR	CIDEr	AP50	mIOU	Recall
Upper Bound, Retain 576 Tokens (100%)											
	100%	16.2	47.2	30.8	66.3	41.8	15.8	43.5	29.2	65.6	40.8
Retain 57 Tokens (\downarrow 90%)											
Fastv	20%	12.6	27.8	14.0	48.1	23.3	13.1	28.3	13.6	47.9	25.1
PDrop	20%	12.8	28.1	15.1	49.7	25.3	12.9	28.7	14.6	59.1	26.8
ALTP	20%	12.4	28.1	20.0	55.5	30.3	12.0	29.0	19.4	54.6	34.4
Retain 144 Tokens (\downarrow 75%)											
Fastv	33%	12.8	30.9	20.9	50.8	30.4	12.7	29.0	20.2	53.8	30.0
PDrop	33%	13.5	31.5	21.7	52.1	31.9	13.1	30.5	21.5	55.2	31.7
ALTP	33%	13.4	31.1	24.8	60.3	34.2	12.4	30.1	23.9	59.7	33.1
Retain 288 Tokens (\downarrow 50%)											
Fastv	55%	13.2	34.3	24.4	61.9	33.2	13.1	32.1	23.3	61.2	32.9
PDrop	55%	13.8	34.1	25.6	62.7	33.9	14.2	33.7	24.1	61.9	33.0
ALTP	55%	13.6	33.7	26.3	62.2	34.9	13.4	33.4	25.1	62.1	34.4

Table 1. Result of our pruning method on Glamm on GrandF dataset under different setting of retain/pruning token ratio. ALTP significantly outperforms Pdrop [27] and Fastv[4] under 75% and 90% token dropping setting.

alongside FastV [4] and PDrop [27] on the Glamm model, evaluated on the GrandF dataset. We assess the models across various token retention ratios, specifically retaining 57, 144, and 288 tokens, corresponding to a 90%, 75%, and 50% reduction in visual tokens, respectively. At the highest compression ratio, retaining only 57 tokens (90% reduction), ALTP achieves remarkable gains in structural understanding metrics. Specifically, ALTP improveS AP50 by **4.9%** (20.0 vs. 15.1) and Recall by **5.0%** (30.3 vs. 25.3) on the Val set compared to PDrop. This performance advantage is even more pronounced when compared to FastV. When retaining 144 tokens (75% reduction), ALTP attain the highest mIOU of 60.3% on Val, outperforming PDrop by **8.2%** (60.3 vs. 52.1) and FastV by **9.5%** (60.3 vs. 50.8). With 288 tokens retained (50% reduction), the performance gap between ALTP and PDrop narrows. Specifically, ALTP achieves 26.3% AP50 and 62.2% mIOU on the validation set, and 25.1% AP50 and 62.1% mIOU on the test set. In summary, though PDrop shows slightly strong performance in captioning metrics, ALTP demonstrates superior performance in visual metrics across varying token retention ratios, particularly at high compression rates.

ALTP perform well with OMG-Llava Table 2 demonstrates the efficacy of ALTP on the OMG-Llava model. With 25 tokens retained (90% reduction), ALTP significantly enhances performance. Specifically, our method improves AP by **2.1%** and mIOU by **3.0%** on the validation set compared to PDrop. On the test set, ALTP improves AP by 1.5% and mIOU by 1.6%. This highlights the superior grounding accuracy and segmentation precision achieved by our approach under high compression. At 64 tokens (75% reduction), ALTP maintains a competitive edge, improving AP by 0.7% on the validation set and 0.6% on the test set, while demonstrating comparable mIOU and Recall

Model Name	Val			Test		
	AP	mIOU	R	AP	mIOU	R ¹
Upper Bound, Retain 576 Tokens (100%)						
	29.9	65.5	43.6	29.2	64.6	42.3
Retain 25 Tokens (\downarrow 90%)						
Pdrop	24.1	58.0	35.4	22.9	57.7	34.1
ALTP	26.2	61.0	37.4	24.4	59.3	35.6
Retain 64 Tokens (\downarrow 75%)						
Pdrop	27.2	63.5	38.7	26.3	63.2	38.6
ALTP	27.9	63.6	39.2	26.9	62.3	39.5

Table 2. Result of our pruning method on OMG-Llava on GrandF dataset under different setting of retain/pruning token ratio. AP, R represent for AP50 and recall respectively. ALTP outperforms Pdrop under 75% and 90% token dropping.

scores. This confirms our method’s ability to preserve crucial visual information for grounded conversation generation, especially under severe token reduction. The potential reason that our method’s performance improvement is more pronounced when applied to Glamm than to OMG-Llava is discussed in Section 5 .

4.3. Module Ablation study

Table 3 presents an ablation study evaluating the impact of our ALTP method’s components, Detail Density Capture (DDC) and Dynamic Density Formation (DDF). At a 90% token reduction (57 tokens), ALTP achieves a 20.0% AP and 55.5% mIOU on the validation set, compared to 18.9% AP and 53.8% mIOU with only DDC. This indicates that DDF contributes a 1.1% improvement in AP and a 1.7% increase in mIOU. On the test set, ALTP improves Recall by 5.0% over only using DDC. With 144 tokens retained

¹Note that the original OMG-Llava paper does not calculate recall metrics. The recall in this table is result from our experiment.

Module name	Val			Test		
	AP	mIOU	R	AP	mIOU	R
Retain 57 Tokens (%)						
Only DDC	18.9	53.8	29.1	18.8	54.2	29.4
ALTP	20.0	55.5	30.3	19.4	54.6	34.4
Retain 144 Tokens (75%)						
Only DDC	24.3	60.1	33.8	23.7	59.2	33.1
ALTP	24.8	60.3	34.2	23.9	59.7	33.1
Retain 288 Tokens (50%)						
Only DDC	25.5	62.1	34.8	24.7	62.1	34.5
ALTP	26.3	62.2	34.9	25.1	62.1	34.6

Table 3. Ablation study showing that while DDC effectively preserves local information, DDF’s dynamic allocation based on information density further improves grounding and segmentation metrics.

(75% reduction), ALTP shows a 0.5% AP and 0.2% mIOU improvement on the validation set, demonstrating that DDF fine-tunes the token distribution for better performance. At 288 tokens (50% reduction), ALTP achieves a 26.3% AP, compared to 25.5% with only DDC, a 0.8% improvement. These results validate that while DDC provides a strong baseline by focusing on local information, DDF further enhances performance by dynamically allocating tokens based on information density.

4.4. Hyperparameter robustness study

Table 4 examines the robustness of our ALTP method to variations in superpixel hyperparameters, specifically the number of areas (N) and compactness (C). When N is set to 3, a significant performance drop is observed, with AP decreasing to 17.1% on both validation and test sets. This occurs because with very few sub-areas, ALTP’s localized pruning reverts to a more global, attention-based approach akin to FastV. Optimal performance is achieved with N=7, yielding the highest AP (20.5% on validation, 19.8% on test) and mIOU (55.9% on validation, 54.8% on test). For C, variations between 3, 5 (default), and 10 show minimal impact, indicating ALTP’s stability across a range of compactness values. This suggests that while the number of sub-areas affects performance, the balance between color and spatial proximity within superpixels is less critical.

5. Discussion

Figure 6 illustrates the attention maps of the middle layers during the decoding process for OMG-Llava and Glamm. Visual analysis reveals a significant disparity in image token attention between the two models when evaluated on the Grandf [23] dataset. Specifically, OMG-Llava’s attention is more concentrated on image tokens corresponding to the image’s center, compared to Glamm. Given that center image regions typically contain more salient objects, pruning methods like Fastv or PDrop naturally retain these central

Hyper-parameter	Val			Test			
	AP	mIOU	R	AP	mIOU	R	
N	3	17.1	53.7	27.1	17.1	51.8	27.6
	7	20.5	55.9	30.8	19.8	54.8	34.7
	10 (Default)	20	55.5	30.3	19.4	54.6	34.4
	15	20.1	55.4	30.6	19.1	54.7	34.3
C	3	20.2	55.3	30.5	19.1	54.5	34.2
	5 (Default)	20	55.5	30.3	19.4	54.6	34.4
	10	19.8	55.7	30.1	19.6	54.4	34.3

Table 4. Analysis of Hyperparameter N (Target Number of Areas) and C (Compactness) on ALTP Performance. The results show ALTP is robust to N from 7 to 15 and C from 3 to 10.

tokens. This tendency partially explains why our method’s performance improvement is more pronounced when applied to Glamm than to OMG-Llava.

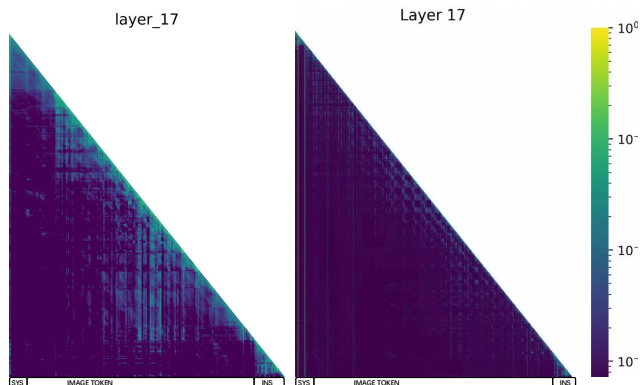


Figure 6. Left: The attention map of OMG-Llava on Grand [22] dataset. Right: The attention map of Llava. We could observe a huge difference among the attention patterns of image tokens.

6. Conclusion

We present Adaptive Local-Aware Token Pruning (ALTP), a novel framework that addresses the computational burden of Grounded Conversation Generation (GCG) models by prioritizing local visual features during token pruning. Our ALTP integrates Detail Density Capture (DDC), which segments images and retains tokens based on regional importance, and Dynamic Density Formation (DDF), which dynamically allocates tokens according to information density. Through extensive experiments on GLaMM and OMG-LLaVA, we demonstrate that ALTP significantly outperforms existing token pruning methods. ALTP provides a promising approach for accelerating GCG models by effectively managing local information crucial for accurate visual grounding.

References

- [1] Radhakrishna Achanta, Appu Shaji, Kevin Smith, Aurelien Lucchi, Pascal Fua, and Sabine Süsstrunk. Slic superpixels compared to state-of-the-art superpixel methods. *IEEE Transactions on Pattern Analysis and Machine Intelligence*, 34(11):2274–2282, 2012. 5
- [2] Jean-Baptiste Alayrac, Jeff Donahue, Pauline Luc, Antoine Miech, Iain Barr, Yana Hasson, Karel Lenc, Arthur Mensch, Katherine Millican, Malcolm Reynolds, et al. Flamingo: a visual language model for few-shot learning. *Advances in neural information processing systems*, 35:23716–23736, 2022. 2
- [3] Keqin Chen, Zhao Zhang, Weili Zeng, Richong Zhang, Feng Zhu, and Rui Zhao. Shikra: Unleashing multimodal llm’s referential dialogue magic. *arXiv preprint arXiv:2306.15195*, 2023. 3
- [4] Liang Chen, Haozhe Zhao, Tianyu Liu, Shuai Bai, Junyang Lin, Chang Zhou, and Baobao Chang. An image is worth 1/2 tokens after layer 2: Plug-and-play inference acceleration for large vision-language models, 2024. 1, 2, 3, 4, 6, 7
- [5] Zhe Chen, Jiannan Wu, Wenhai Wang, Weijie Su, Guo Chen, Sen Xing, Muyan Zhong, Qinglong Zhang, Xizhou Zhu, Lewei Lu, Bin Li, Ping Luo, Tong Lu, Yu Qiao, and Jifeng Dai. Internvl: Scaling up vision foundation models and aligning for generic visual-linguistic tasks, 2024. 1
- [6] Zhe Chen, Weiyun Wang, Yue Cao, Yangzhou Liu, Zhangwei Gao, Erfei Cui, Jinguo Zhu, Shenglong Ye, Hao Tian, Zhaoyang Liu, Lixin Gu, Xuehui Wang, Qingyun Li, Yimin Ren, Zixuan Chen, Jiapeng Luo, Jiahao Wang, Tan Jiang, Bo Wang, Conghui He, Botian Shi, Xingcheng Zhang, Han Lv, Yi Wang, Wenqi Shao, Pei Chu, Zhongying Tu, Tong He, Zhiyong Wu, Huipeng Deng, Jiaye Ge, Kai Chen, Kaipeng Zhang, Limin Wang, Min Dou, Lewei Lu, Xizhou Zhu, Tong Lu, Dahua Lin, Yu Qiao, Jifeng Dai, and Wenhai Wang. Expanding performance boundaries of open-source multimodal models with model, data, and test-time scaling, 2025. 1
- [7] Yong Xien Chng, Henry Zheng, Yizeng Han, Xuchong Qiu, and Gao Huang. Mask grounding for referring image segmentation, 2024. 1
- [8] Sahar Kazemzadeh, Vicente Ordonez, Marc andre Matten, and Tamara L. Berg. Referitgame: Referring to objects in photographs of natural scenes. In *Conference on Empirical Methods in Natural Language Processing*, 2014. 6
- [9] Alexander Kirillov, Eric Mintun, Nikhila Ravi, Hanzi Mao, Chloe Rolland, Laura Gustafson, Tete Xiao, Spencer Whitehead, Alexander C Berg, Wan-Yen Lo, et al. Segment anything. In *Proceedings of the IEEE/CVF international conference on computer vision*, pages 4015–4026, 2023. 1, 3, 4
- [10] Xin Lai, Zhuotao Tian, Yukang Chen, Yanwei Li, Yuhui Yuan, Shu Liu, and Jiaya Jia. Lisa: Reasoning segmentation via large language model. In *Proceedings of the IEEE/CVF Conference on Computer Vision and Pattern Recognition*, pages 9579–9589, 2024. 3, 6
- [11] Xin Lai, Zhuotao Tian, Yukang Chen, Yanwei Li, Yuhui Yuan, Shu Liu, and Jiaya Jia. Lisa: Reasoning segmentation via large language model, 2024. 1
- [12] Junnan Li, Dongxu Li, Silvio Savarese, and Steven Hoi. Blip-2: Bootstrapping language-image pre-training with frozen image encoders and large language models. In *International conference on machine learning*, pages 19730–19742. PMLR, 2023. 2
- [13] Haotian Liu, Chunyuan Li, Qingyang Wu, and Yong Jae Lee. Visual instruction tuning, 2023. 2
- [14] Haotian Liu, Chunyuan Li, Qingyang Wu, and Yong Jae Lee. Visual instruction tuning, 2023. 1, 4
- [15] Haotian Liu, Chunyuan Li, Yuheng Li, and Yong Jae Lee. Improved baselines with visual instruction tuning. In *Proceedings of the IEEE/CVF Conference on Computer Vision and Pattern Recognition*, pages 26296–26306, 2024. 2
- [16] Shilong Liu, Zhaoyang Zeng, Tianhe Ren, Feng Li, Hao Zhang, Jie Yang, Qing Jiang, Chunyuan Li, Jianwei Yang, Hang Su, et al. Grounding dino: Marrying dino with grounded pre-training for open-set object detection. In *European Conference on Computer Vision*, pages 38–55. Springer, 2024. 3
- [17] Kenneth Marino, Mohammad Rastegari, Ali Farhadi, and Roozbeh Mottaghi. Ok-vqa: A visual question answering benchmark requiring external knowledge, 2019. 1
- [18] Xuran Pan, Tianzhu Ye, Zhuofan Xia, Shiji Song, and Gao Huang. Slide-transformer: Hierarchical vision transformer with local self-attention, 2023. 2
- [19] Zhiliang Peng, Wenhui Wang, Li Dong, Yaru Hao, Shaohan Huang, Shuming Ma, and Furu Wei. Kosmos-2: Grounding multimodal large language models to the world. *arXiv preprint arXiv:2306.14824*, 2023. 3
- [20] Qwen, ., An Yang, Baosong Yang, Beichen Zhang, Binyuan Hui, Bo Zheng, Bowen Yu, Chengyuan Li, Dayiheng Liu, Fei Huang, Haoran Wei, Huan Lin, Jian Yang, Jianhong Tu, Jianwei Zhang, Jianxin Yang, Jiaxi Yang, Jingren Zhou, Junyang Lin, Kai Dang, Keming Lu, Keqin Bao, Kexin Yang, Le Yu, Mei Li, Mingfeng Xue, Pei Zhang, Qin Zhu, Rui Men, Runji Lin, Tianhao Li, Tianyi Tang, Tingyu Xia, Xingzhang Ren, Xuancheng Ren, Yang Fan, Yang Su, Yichang Zhang, Yu Wan, Yuqiong Liu, Zeyu Cui, Zhenru Zhang, and Zihan Qiu. Qwen2.5 technical report, 2025. 1
- [21] Alec Radford, Jong Wook Kim, Chris Hallacy, Aditya Ramesh, Gabriel Goh, Sandhini Agarwal, Girish Sastry, Amanda Askell, Pamela Mishkin, Jack Clark, Gretchen Krueger, and Ilya Sutskever. Learning transferable visual models from natural language supervision, 2021. 4
- [22] Hanoona Rasheed, Muhammad Maaz, Sahal Shaji Mulla-pillay, Abdelrahman Shaker, Salman Khan, Hisham Cholakkal, Rao M. Anwer, Erix Xing, Ming-Hsuan Yang, and Fahad S. Khan. Glamm: Pixel grounding large multimodal model, 2024. 1, 2, 3, 6, 8
- [23] Yuzhang Shang, Mu Cai, Bingxin Xu, Yong Jae Lee, and Yan Yan. Llava-prumerge: Adaptive token reduction for efficient large multimodal models, 2024. 4
- [24] Wenhai Wang, Zhe Chen, Xiaokang Chen, Jiannan Wu, Xizhou Zhu, Gang Zeng, Ping Luo, Tong Lu, Jie Zhou, Yu Qiao, et al. Visionllm: Large language model is also an open-ended decoder for vision-centric tasks. *Advances in Neural Information Processing Systems*, 36:61501–61513, 2023. 3

- [25] Zhiyu Wu, Xiaokang Chen, Zizheng Pan, Xingchao Liu, Wen Liu, Damai Dai, Huazuo Gao, Yiyang Ma, Chengyue Wu, Bingxuan Wang, Zhenda Xie, Yu Wu, Kai Hu, Jiawei Wang, Yaofeng Sun, Yukun Li, Yishi Piao, Kang Guan, Aixin Liu, Xin Xie, Yuxiang You, Kai Dong, Xingkai Yu, Haowei Zhang, Liang Zhao, Yisong Wang, and Chong Ruan. Deepseek-vl2: Mixture-of-experts vision-language models for advanced multimodal understanding, 2024. [1](#)
- [26] Zhuofan Xia, Dongchen Han, Yizeng Han, Xuran Pan, Shiji Song, and Gao Huang. Gsva: Generalized segmentation via multimodal large language models, 2024. [1](#)
- [27] Long Xing, Qidong Huang, Xiaoyi Dong, Jiajie Lu, Pan Zhang, Yuhang Zang, Yuhang Cao, Conghui He, Jiaqi Wang, Feng Wu, and Dahua Lin. Pyramidrop: Accelerating your large vision-language models via pyramid visual redundancy reduction, 2025. [1](#), [4](#), [6](#), [7](#)
- [28] Xiang Yue, Yuansheng Ni, Kai Zhang, Tianyu Zheng, Ruoqi Liu, Ge Zhang, Samuel Stevens, Dongfu Jiang, Weiming Ren, Yuxuan Sun, Cong Wei, Botao Yu, Ruibin Yuan, Renliang Sun, Ming Yin, Boyuan Zheng, Zhenzhu Yang, Yibo Liu, Wenhao Huang, Huan Sun, Yu Su, and Wenhui Chen. Mmmu: A massive multi-discipline multimodal understanding and reasoning benchmark for expert agi, 2024. [1](#)
- [29] Shilong Zhang, Peize Sun, Shoufa Chen, Min Xiao, Wenqi Shao, Wenwei Zhang, Kai Chen, and Ping Luo. Gpt4roi: Instruction tuning large language model on region-of-interest. *arXiv preprint arXiv:2307.03601*, 2023. [3](#)
- [30] Tao Zhang, Xiangtai Li, Hao Fei, Haobo Yuan, Shengqiong Wu, Shunping Ji, Chen Change Loy, and Shuicheng Yan. Omg-llava: Bridging image-level, object-level, pixel-level reasoning and understanding, 2024. [1](#), [3](#), [6](#)
- [31] Yuan Zhang, Chun-Kai Fan, Junpeng Ma, Wenzhao Zheng, Tao Huang, Kuan Cheng, Denis Gudovskiy, Tomoyuki Okuno, Yohei Nakata, Kurt Keutzer, and Shanghang Zhang. Sparsevlm: Visual token sparsification for efficient vision-language model inference, 2025. [4](#), [6](#)
- [32] Yang Zhao, Zhijie Lin, Daquan Zhou, Zilong Huang, Jiashi Feng, and Bingyi Kang. Bubogpt: Enabling visual grounding in multi-modal llms. *arXiv preprint arXiv:2307.08581*, 2023. [3](#)
- [33] Yuke Zhu, Chi Xie, Shuang Liang, Bo Zheng, and Sheng Guo. Focusllava: A coarse-to-fine approach for efficient and effective visual token compression, 2024. [4](#), [6](#)